Solution-processed finger-type organic proximity sensor with high displacement resolution

Jung-Sung Liao[1], Kuan-Hsun Wang[1], Hsiao-Wen Zan[1]*, Hsin-Fei Meng[2]*, Ping-Hung Yeh[3], Chuang-Chuang Tsai[1]
[1] Department of Photonics and Institute of Electro-Optics, National Chiao Tung University, Hsinchu, Taiwan
[2] Institute of Physics, National Chiao Tung University, Hsinchu, Taiwan
[3] Department of Physics, Tamkang University, New Taipei City, Taiwan
* Email:hsiaowen@mail.nctu.edu.tw, meng@mail.nctu.nctu.edu.tw

Wilfried Hortschitz[4], Harald Steiner[4], Thilo Sauter[4,5]*
[4] Center for Integrated Sensor Systems, Danube University Krems, Wiener Neustadt, Austria
[5] Institute of Computer Technology, TU Wien, Vienna, Austria
* Email:Thilo.sauter@donau-uni.ac.at

***Abstract*—Proximity sensors are interesting devices for applications like smart homes or human-machine interfaces. This work investigates a cheap and compact short-range proximity sensor based on an organic photo detector combined with a commercial LED. Low-cost solution-processed organic materials are used, and low process temperatures at 140 ºC also facilitate future integration on, e.g., plastic substrates. In particular, to avoid damage of the organic layer during the patterning process, a new organic photo detector with a semi-transparent organic active layer and a transparent silver nanowire top electrode was designed. The proposed sensor can be realized by using only one shadow mask to pattern the opaque bottom electrode layer. The opaque finger-type bottom electrode not only partly shields the light emitted from below the device, but also defines the active regions with vertical electric field to generate and collect photo current. In the experiments conducted in this paper, the maximum detection distance was found to be 2 cm, whereas the lower end of the measurement range was 0.2 cm.**

Keywords—finger-type photodetector; OPD; proximity sensor;

I. INTRODUCTION

In an increasingly networked and "cyberphysical" world, simple and easy-to-use interfaces between humans and the computerized environment are becoming more and more important to capture and track interaction. Other than cameras which are expensive and raise privacy concerns, proximity sensors are interesting means to detect presence of humans or objects. Cost-effectiveness and ease of deployment allow for distributed application as smart networked sensors in a multitude of scenarios including smart homes, healthcare, or factory automation [1-2].

Proximity sensors can be implemented based on several physical principles. Prominent examples are ultrasound sensors which are popular in automotive and industrial applications, or infrared sensors often used in building surveillance [3-8]. Another possibility, which is the focus of this paper, is to use an optical principle based on the detection of light reflected from an object close to the sensor. Arranging light transmitter and receiver in a coplanar setup facilitates system integration and practical use. Such devices can be used as human-machine interfaces and can detect small distance variations [9]. In previous work, we combined polymer light-emitting diodes (PLED) and a polymer photodiode to an optical proximity sensor in the near infrared range [10-11]. The maximum detection distance under normal incidence is almost 20 cm for white paper, Styrofoam, and aluminum foil. However, this setup has a smaller short range sensitivity because the optical axes of LED and detector are spaced apart (Fig. 1(a)). Objects in close proximity of the sensor surface might therefore not reflect sufficient light.

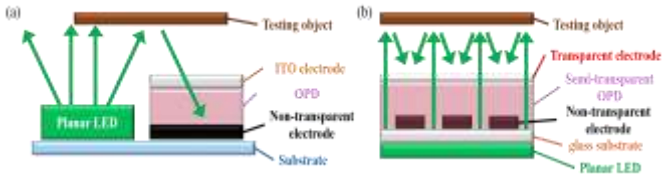

Fig. 1. Schematic setup of the combination of an LED with (a) a standard-type OPD and (b) a finger-type OPD

Sensitivity to lateral displacement at short distances between sensor and object can be made smaller by interleaving light source and detector. This will have the additional benefit of allowing for smaller, highly integrated devices that can also be combined with MEMS elements [12]. As a first step towards such an interleaved structure, this paper investigates the use of an organic photo detector (OPD) as proximity sensor. The basic idea is to fabricate a semi-transparent detector with a finger structure that can be placed on top of a planar LED (Fig. 1(b)). Light emitted from the LED passes through the semi-transparent layer of the OPD stack and is reflected back from the object to the active part of the OPD. The active part of the OPD is confined inside the regions with overlapping top and bottom electrodes. The bottom finger-type electrode is opaque. Hence, in principle, these active parts only react to the reflected light, not to the light emitted from below. For those regions without bottom electrode (inactive parts), the

emitted light does generate certain excitons when passing through these semi-transparent areas. However, without the vertical electric field, no effective photo current can be generated in these inactive parts. Challenges to be met are the fabrication of the finger structure and the avoidance of irradiance "short circuits" within the layers.

The rest of the paper is structured as follows: Sec. II presents the technology used to fabricate both a conventional OPD and the modifications used for the finger-type structure. Sec. III describes the characterization results of the devices using different light sources. Sec. IV investigates the sensitivity to displacement of the finger-type OPD operated as proximity sensor. Finally, sec. V presents a brief conclusion and future work.

II. FABRICATION TECHNOLOGY

A. *Standard-type OPD*

The schematic structure and energy band diagram of the solution-processed standard-type OPD are shown in Figs. 2(a) and 2(b), respectively. The material of the active layer is a donor-acceptor blended system using poly (3-hexylthiophene-2,5-diyl) (P3HT) and n-type [6,6]-phenyl C61-butyric acid methyl ester (PCBM). This combination can be used to create photo-detectors with adjustable response range. The P3HT:PCBM blend is generally very popular in polymer solar cells and photo detectors due to its high sensitivity in the visible range [13]. The fabrication process of this standard-type OPD is shown in Fig. 3. On a glass substrate, indium-tin-oxide (ITO) is used as transparent bottom electrode. The thickness of the ITO layer is 200 nm, and its sheet resistance is lower than 7 Ω/square. The total thickness of the glass substrate is 0.7 mm.

First of all, the ITO layer is etched to form the electrode pattern, then cleaned, and the glass substrate is put into an reactive-ion etching (RIE) O2 plasma system. By plasma treatment, residual small particles can be removed. On the other hand, the work function of ITO is lowered, which provides a better film quality in the following process steps and improves carrier injection. After cooling down to room temperature, poly (3,4-ethylenedioxythiophene) (PEDOT) solution is filtered through a 0.22 μm syringe filter and spin-coated at 3500 rpm on the substrate. The thickness of the PEDOT layer is about 40 nm. Subsequently, the substrate is baked on a hotplate at 200 ºC in atmospheric environment for 15 minutes.

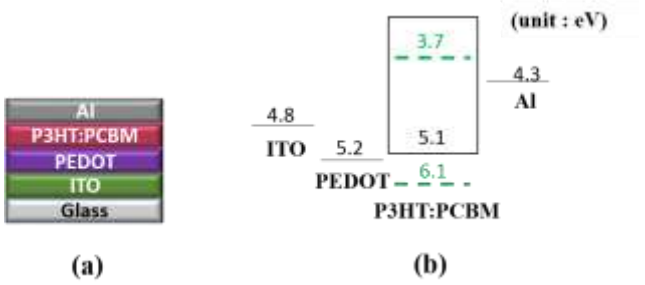

Fig. 2. (a) Schematic structure of the standard-type OPD. (b) Energy band diagram of the standard-type OPD.

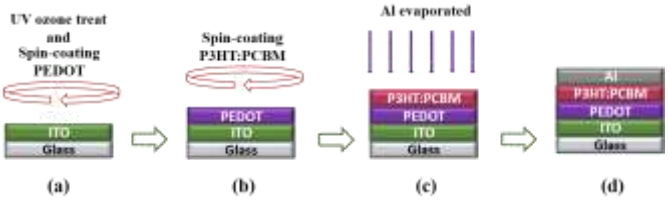

Fig. 3. The fabrication process of the standard-type OPD.

As material for the active layer, a 1:1 mixture by weight of P3HT:PCBM is used. The concentration of P3HT:PCBM solution is 1.7 wt% dissolved in dichlorobenzene and spin coated in two steps using 600 rpm spin rate for 40 seconds at first and 1200 rpm for 3 seconds in the second spin. This results in a thickness of this layer of about 200 nm. Then, the film is slowly dried for 30 minutes before being annealed on a hotplate at 140 ºC for 20 minutes in nitrogen environment. Finally, a 100 nm Al electrode is evaporated on the top of the active layer by thermal evaporation. This standard-type OPD works as photo diode and can receive incident light only from the bottom because the top Al electrode is opaque. To implement the detector structure sketched in Fig. 1(b), however, a layer stack has to be found that is transparent from both sides.

B. *Finger-type OPD*

The basic idea of the finger-type version of the photo detector is to have slices of the standard-type detector and separate them by transparent sections, so that light can pass from a planar backlight and be reflected from an object onto the detector slices. Starting from the standard layer structure, the strategy is to turn the stack upside down and open the Al electrode. The schematic structure is shown in Fig. 4(a). The energy band diagram of the solution-processed finger-type OPD is shown in Fig. 4(b). The material of the active layer is again P3HT:PCBM. Fig.4(c) depicts the absorption spectrum of the P3HT:PCBM active layer. We see that P3HT:PCBM has high absorption at green light.

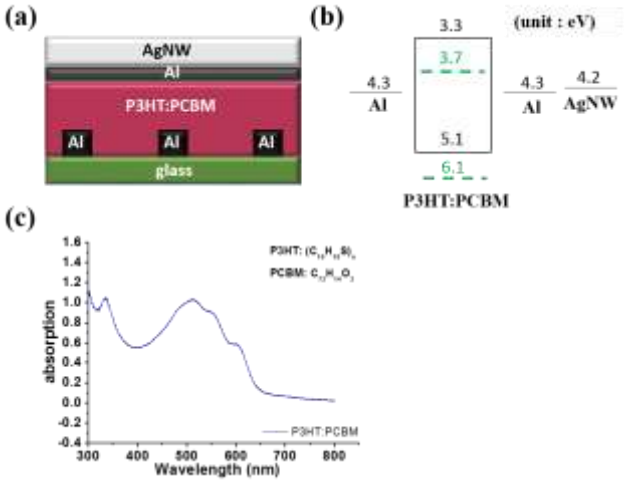

Fig. 4. (a) The schematic structure of the finger-type OPD. (b) The energy band diagram of the finger-type OPD. (c) The absorption spectrum of P3HT:PCBM.

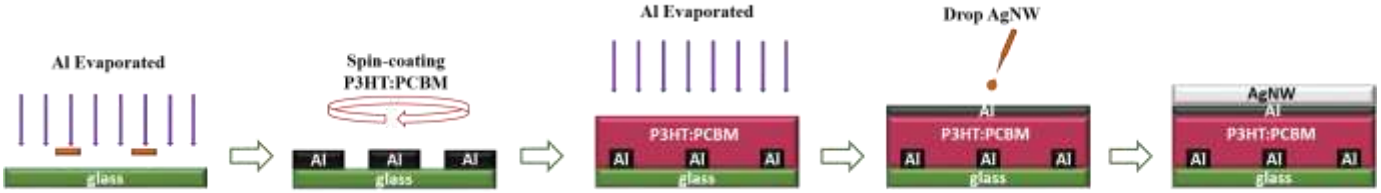

Fig. 5. Fabrication steps of finger-type OPDs

The fabrication process of a finger-type OPD is sketched in Fig. 5. Again, we use glass as the substrate. Based on the specific pattern of the electrode stripes, it is necessary to use thermal evaporation to create the bottom electrode. The process steps are as follows:

- A 100 nm thick Aluminum layer is evaporated through a particular shadow mask. The material for the active layer is, as in the standard case, a 1:1 mixture by weight of P3HT:PCBM. The concentration of P3HT:PCBM solution is 1.7 wt% dissolved in dichlorobenzene and stirred at 60ºC for 24 hours to obtain a uniform solution.
- Then, P3HT:PCBM is spin coated on the substrate with a speed of 600 rpm for 40 seconds in the first step and 1200 rpm for 3 seconds in a second step. Afterwards, the P3HT:PCBM layer is annealed at 140 ºC for 20 minutes in nitrogen environment to improve its electrical characteristic.
- After annealing, 2 nm Aluminum are evaporated on the P3HT:PCBM layer through a shadow mask.
- Finally, Silver nanowires (AgNW) (supplied by Nanostructure & Amorphous Materials Inc.) suspended in isopropanol (IPA) with a concentration 0.03125 wt% are dropped on the surface at a device temperature of 60ºC, as top electrode.

The transmittance of the Al and AgNW combination is 85 %, so that light can sufficiently pass. Contrary to the standard-type OPD, ITO is not used as top electrode because the sputtering process will damage the underlying organic layer.

III. Characterization of the Detector Devices

A. *Standard-type OPD*

In this study, all measurements had to be done in the nitrogen atmosphere. For device characterization of the organic photo detectors, the current density versus voltage (J-V) diagrams were determined. The devices were reverse biased and exposed to light from a conventional ring lamp commonly used as light source for microscopes. The light source irradiates the device from the glass side as shown in Fig. 6. The dark current density and light current density are about 10^{-3} mA/cm^2 and 1 mA/cm^2, respectively. These values are used as benchmark for the finger-type devices.

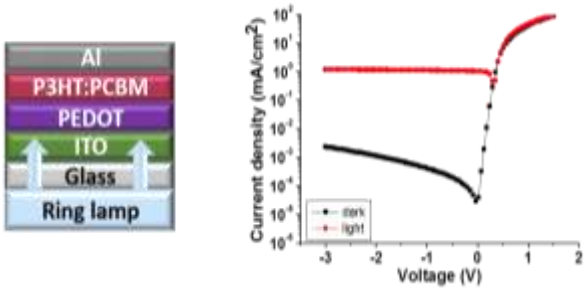

Fig. 6. The schematic diagram and J-V curve of standard-type OPD.

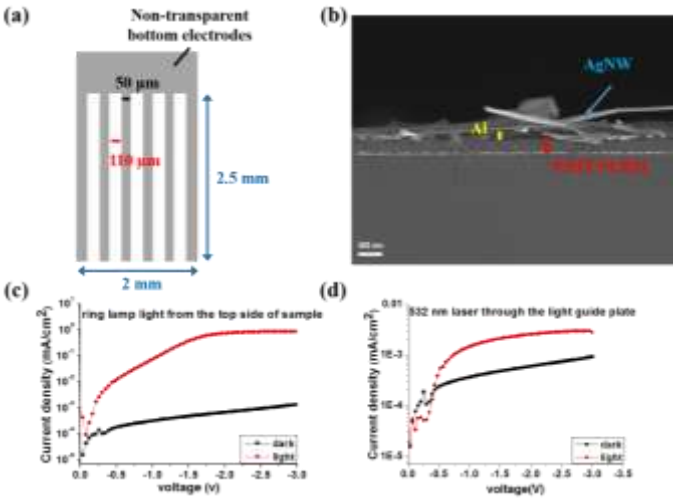

Fig. 7. (a) Schematic structure of the bottom-electrode stripes. (b) SEM picture of the finger-type OPD. (c) J-V curve of the finger-type OPD measured with a ring lamp light source from the top side of the device. (d) J-V curve of the finger-type OPD obtained using a 532 nm laser and a light guide plate from the bottom side of the device.

B. *Finger-type OPD*

Fig. 7(a) shows the structure of the electrode stripes. For the experiments, devices with a size of 2.5 mm x 2 mm were fabricated, such that 50 µm x 2 mm stripes were connected in parallel. The width and the period of the bottom electrode are 50 µm and 110 µm, respectively. Fig. 7(b) shows a Scanning Electron Microscopy (SEM) picture of the finger-type OPD detailing the layer structure. Fig. 7(c) presents the J-V curves measured with the ring lamp irradiated from the top side of the devices, that is to say, through the AgNW / Al electrode. This is the "normal" direction of operation, comparable to the irradiation of the standard-type OPD

through the bottom electrode.

The measurement results show that the dark current density and light current density of the finger-type OPD are about 10^{-3} mA/cm^2 and 1 mA/cm^2, respectively. The current density levels are thus the same as for the standard-type OPD. However, the noticeable difference is that a sufficient reverse bias voltage of about 2 V must be applied in order to reach the saturation value for the light current. This may be explained by the different energy band diagrams of standard-type and finger-type OPDs. As shown in Fig. 2(b), for standard-type OPD, the Fermi level of the two electrodes (ITO/PEDOT and Al) are about 0.5 eV different. Hence, under thermal equilibrium with a unified Fermi level, there are a built-in potential and thus a built-in electric field inside the active layer. The built-in electric field facilitates the conduction of photo-induced carriers and hence a significant photo current can be observed under a small reverse bias. For finger-type OPD, there is no such built-in electric field due to the work function difference between two electrodes (Fig. 4(b)). As a result, increasing the reverse bias from 0 V to 2 V effectively enhances the electric field and the photo current.

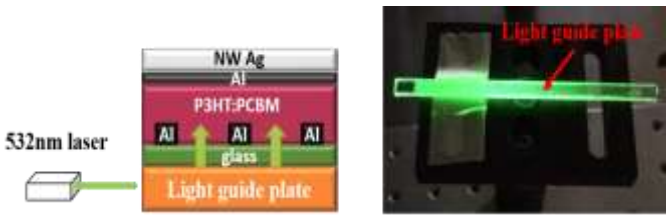

Fig. 8. Schematic diagram of a finger-type OPD measured by a 532 nm laser irradiating into a light guide plate.

In Fig. 7(d), we apply a different light source to characterize the finger-type OPD from the bottom side of the device. The schematic diagram of the device irradiated by a 532 nm laser via a light guide plate is shown in Fig. 8. The light guide plate was made from polymethyl methacrylate (PMMA). The dark current density level in this experiment is evidently the same as in the experiment with the ring lamp and comparable to the standard-type OPD. However, the light current density is lower than using the ring lamp as light source, which is not unexpected because we illuminate the device from the bottom and the Al bottom electrodes largely shield the active part of the device (which is right above the electrodes). The contribution to the light current therefore stems from scattered light inside the P3HT:PCBM layer and partial reflections from the not fully transparent top electrodes.

IV. Finger-type OPD as Proximity Sensor

A. *Experimental setup*

For operating the photo detector as proximity sensor in a more realistic setup, LEDs were chosen as light source. Specifically, commercial white and green LEDs were applied considering the spectral sensitivity of the OPD. The used white LED (3.2 Vf, 15000 mcd) was LA-504W3CA-1C-01, the green LED (3.2 Vf, 12000 mcd) was LA-503G6CA-3C-01. The measurement equipment set-up is shown in Fig. 9. The LED light source will irradiate through a hole. The hole size is the same as the active region. The reflective plate was fabricated by evaporating 100 nm Aluminum on a glass substrate. A precision fine tuning platform was used to control the displacement of the reflective plate.

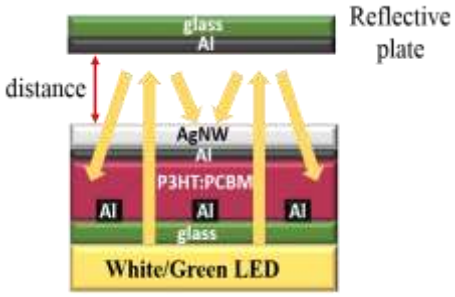

Fig. 9. Schematic diagram of the finger-type OPD operated as proximity sensor with white and green LED light sources.

For the experiments, the distance between the reflective plate and the samples varied from 0.3 cm, 0.5 cm, 1 cm, 1.3 cm, to 2 cm. The dark current density was measured for comparison. The diode current density as a function of bias voltage (J-V curves) of the finger-type OPD using green and white LED light sources are shown in Figs. 10(a) and (b), respectively. The results demonstrate that it is possible to detect small up and down displacements. It should be noted that when the distance is 2 cm, the obtained current is the same as the current without the reflective plate. Hence, in this setup, the maximum detectable distance is only 2 cm. Increasing the spacing in the finger structure can however be expected to increase also the detectable distance. In future work, a wide and tunable detecting range may therefore be achieved by using sensors with different finger spacing.

B. *Sensitivity to displacement*

The results in Fig. 10 show that the sensitivity of the device depends on the bias voltage. Fig. 11 presents a different view to the experimental data. It shows that the difference of light and dark current density is linear in the distance range from 0.2 cm to 2 cm when the reverse bias voltage is higher than 1 V. For distances larger than 2 cm, the current density does not decrease significantly, which again indicates that the maximum detection distance for the given setup is 2 cm. The smallest displacement that can be detected by the finger-type OPD is 0.2 cm. Within this range, the displacement can be precisely measured. Evidently, higher reverse bias yields higher currents and thus higher sensitivity.

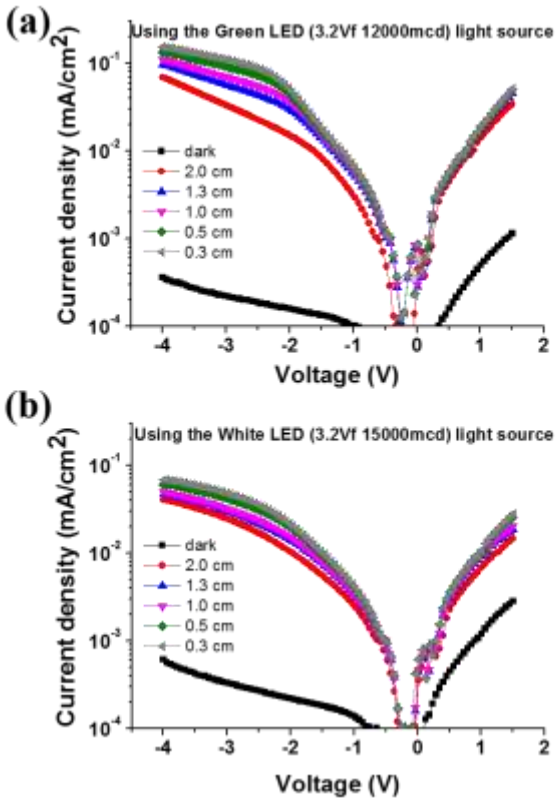

Fig. 10. J-V curves of the finger-type OPD measured with different distance of the reflective plate for (a) green LED and (b) white LED light sources.

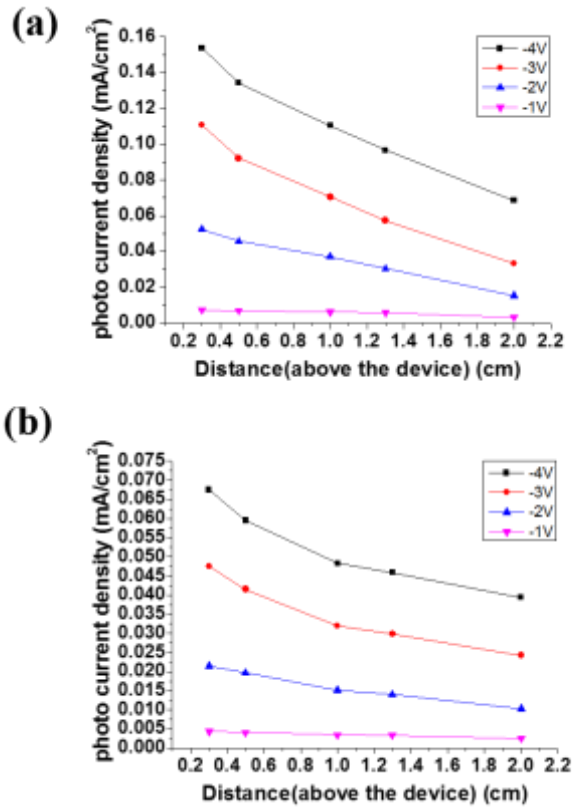

Fig. 11. Dependence of the photo current density on the distance of the reflective plate above the device at different bias voltages and with different light sources. (a) Green LED as light source. (b) White LED as light source.

The effective photo current densities shown in Fig. 11 were calculated as the current density under irradiation minus the current density in the dark. The photo current densities as a function of the distance by using green LED and white LED are shown in Fig. 11(a) and Fig. 11(b), respectively. It can clearly be seen that using the green LED light source results in higher photo current density than using the white LED for the same variation of displacement. The OPD is sensitive toward green light, as shown in Fig. 4(d), since the absorption wavelength of P3HT:PCBM is near the green part of the spectrum.

White LEDs, on the other hand, have only a small part of their spectrum in this range, hence only a small part of the irradiated light is usable for the OPD. For future studies, green light sources will therefore be preferable. Regarding the sensitivity, we can conclude that the distance range of [0.5 cm, 2 cm] above the device exhibits a reasonably linear characteristic and will thus be the focus of interest in subsequent experiments.

V. Conclusion and Future Work

Proximity sensors are useful devices for cyberphysical systems and human-machine interfaces. In this study, we investigated first technological steps towards highly integrated, short-range proximity sensors based on organic optical devices. Specifically, we successfully fabricated and characterized a finger-type organic photo detector as array. Using commercial green or white LEDs as light sources, the finger-type OPD as a proximity sensor was shown to detect small up and down displacements. The maximum detection distance was found to be 2 cm in the setup studied in this paper, whereas the smallest variation of displacement that can be detected was 0.2 cm. In accordance with the spectral sensitivity of the OPD, experiments showed that the optimum light source is a green LED.

Future research will investigate how to extend the measurement range. As already discussed in the previous section, varying the spacing of the fingers can increase the usable range. Furthermore, ways to reduce the spurious internal reflections inside the active layer will be sought to lower the detection limit. Finally, attention will also be devoted to material considerations. In this study, all measurements had to be done in the nitrogen atmosphere because the organic materials are sensitive to moisture and

oxygen. In future work, other materials [14-15] can be investigated to fabricate air-stable OPDs. Alternatively, methods for effective protective coating can be tested to cope with lifetime issues of the organic devices.

Acknowledgment

This work was partly carried out within the scope of the M-ERA.net project COSiFlex funded by the Taiwanese Ministry of Science and Technology (MOST, project number 103-2120-M-009 -008) and the Austrian Research Promotion Agency (FFG, project number 846174).

References

[1] M. Kovatsch, S. Mayer, and B. Ostermaier, "Moving Application Logic from the Firmware to the Cloud: Towards the Thin Server Architecture for the Internet of Things," IMIS, 2012.

[2] L. Atzori, A. Lera, and G. Morabito, "From "Smart Objects" to "Social Objects": The Next Evolutionary Step of the Internet of Things," Communications Magazine, IEEE, vol. 52, Issue 1, 2014, pp. 97-105.

[3] W. Manthey, N. Kroemer, and V. Magorl, "Ultrasonic transducers and transducer arrays for applications in air," Meas. Sci. Technol., vol. 3, 1992, pp. 249-261.

[4] J.D. Turner and L. Austin, "Sensors for automotive telematics," Meas. Sci. Technol., vol. 11, 2000, pp. 58-79.

[5] J. Oria and A.M.G. Gonzalez, "Object recognition using ultrasonic sensors in robotic applications," IEEE Conference on Industrial Electronics, Control, and Instrumentation, vol. 3, 1993, pp.1927-1931.

[6] R.C. Luo, "Sensor Technologies and Microsensor Issues for Mechatronics Systems," IEEE/ASME Transactions on Mechatronics, vol. 1, 1996, pp. 39-49.

[7] P. Zappi, E. Farella, and L.B. Fellow, " Tracking Motion Direction and Distance With Pyroelectric IR Sensors," IEEE Sensors Journal, vol. 10, Issue 9, 2010, pp. 1486-1494.

[8] P. Zappi, E. Farella, and L. Benini, "Pyroelectric InfraRed Sensors Based Distance Estimation," IEEE Sensors, 2008, pp. 716-719.

[9] H.T. Cheng, A.M. Chen, A. Razdan, and E. Buller, "Contactless Gesture Recognition System Using Proximity Sensors," Consumer Electronics (ICCE), IEEE International Conference on, 2011, pp. 149-150.

[10] E.C. Chen, S.R. Tseng, J.H. Ju, C.M. Yang, H.F. Meng, S.F. Horng, and C.F. Shu, "Polymer Infrared Proximity Sensor," Appl. Phys. Lett., vol. 93, 2008, 063304.

[11] E.C. Chen, C.Y. Shih, M.Z. Dai, H.C. Yeh, Y.C. Chao, H.F. Meng, H.W. Zan, W.R. Liu, Y.C. Chiu, Y.T. Yeh, C.J. Sun, S.F. Horng, and C.F. Shu, "Polymer Infrared Proximity Sensor," IEEE Transactions on Electron Devices, vol. 58, NO. 4, 2011.

[12] T. Sauter, W. Hortschitz, H. Steiner, M. Stifter, C. Hsin, H.W. Zan, H. Meng, and P. Chao, "Making optical MEMS sensors more compact using organic light sources and detectors," IEEE Conference on Emerging Technologies & Factory Automation (ETFA), Barcelona, 16.-19. Sep. 2014, pp. 1-4.

[13] G. Yu, J. Gao, J.C. Hummelen, F. Wudl, and A.J. Heeger, "Polymer Photovoltaic Cells: Enhanced Efficiencies via a Network of Internal Donor-Acceptor Heterojunctions," Science, vol. 270, 1995, pp. 1789-1791.

[14] M. Binda, T. Agostinelli, M. Caironi, D. Natali, M. Sampietro, L. Beverina, R. Ruffo, and F. Silvestri, "Fast and air stable near-infrared organic detector based on squaraine dyes," ScienceDirect, vol. 10, Issue 7, 2009, pp. 1314-1319.

[15] K.J. Baeg, M. Binda, D. Natali, M. Caironi, and Y.Y. Noh, "Organic Light Detectors: Photodiodes and Phototransistors," Adv. Mater., vol. 25, 2013, pp. 4267-429